

## Supporting Information

### **Novel Small-Molecule Electron-Donor for Solution Processed Ternary Exciplex with 24% External Quantum Efficiency in Organic Light-Emitting Diode**

*Juewen Zhao, Caijun Zheng,\* Yu Zhou, Chuan Li, Jun Ye,\* Xiaoyang Du, Wan Li, Zeyu He, Ming Zhang, Hui Lin, Silu Tao\* and Xiaohong Zhang*

### **List of Contents**

**SI-1. Synthesis of TPA-3**

**SI-2. Photophysical properties of TPA-3**

**SI-3. Low temperature (77 K) phosphorescence spectrum**

**SI-4. HOMO, LUMO, and excited state energies**

**SI-5. Vacuum deposited devices**

**SI-6. Investigation on turn voltage**

**SI-7. Photophysical properties of 3CzFDPhTz:PO-T2T and 9PhFDPhTz:PO-T2T**

**SI-8. Calculation of rate constants of different kinetic processes**

**SI-9. <sup>1</sup>H NMR and <sup>13</sup>C NMR spectra of TPA-3**

## SI-1. Synthesis of TPA-3

### Synthesis of 4-(9H-fluoren-9-yl)-N,N-diphenylaniline (3)

A sample of 0.18 g 9-fluorenone (1) (1.0 mmol) was dissolved into 10 mL toluene at room temperature. Then 0.28 g *p*-toluenesulfonyl hydrazide (1.5 mmol) was added and the mixture was heated up to 80 °C. After stirring for 2 h, 0.28 g potassium carbonate (K<sub>2</sub>CO<sub>3</sub>, 2.0 mmol) and 0.43 g (4-(diphenylamino)phenyl)boronic acid (2) (1.5 mmol) were added, giving a color change immediately. The reaction was further stirred for 5 h at 110 °C before quenched by water (20 mL) and extracted by CH<sub>2</sub>Cl<sub>2</sub> (3×20 mL). The organic layer was dried with anhydride Na<sub>2</sub>SO<sub>4</sub> and the solvent was removed in vacuo. The residue was purified by flash column chromatography with eluent of petroleum ether and CH<sub>2</sub>Cl<sub>2</sub> (10:1) to give a white solid (yield 75%). <sup>1</sup>H NMR (400 MHz, CDCl<sub>3</sub>, δ): 7.77 (s, 2H), 7.37 (d, *J* = 8.2 Hz, 4H), 7.27 (s, 2H), 7.18 (s, 4H), 7.12 - 7.02 (m, 4H), 6.93 (s, 6H), 4.98 (s, 1H). HRMS (ESI) *m/z*: [M + H<sup>+</sup>] calcd for C<sub>31</sub>H<sub>23</sub>N 409.1830, found 410.1824.

### Synthesis of TPA-3

In N<sub>2</sub>, 0.40 g compound 3 (1.0 mmol) was dissolved in 5 ml anhydrous tetrahydrofuran (THF). The solution was cooled to -78 °C and *n*-BuLi (1.6 M in hexane, 1.3 mmol) was added dropwisely. The mixture was stirred for 2 h at -78 °C in order to fully form the lithium salts, a crucial nucleophile for the next step. Then 0.25 g perfluoropyridine (4) (1.5 mmol) in dry THF was added with syringe at the same temperature. The system was allowed to warm up to room temperature slowly. After stirred at room temperature for 3 h, the reaction was quenched by water addition. The mixture was extracted with CH<sub>2</sub>Cl<sub>2</sub> (3×30 mL). The organic phase was combined and dried with anhydrous Na<sub>2</sub>SO<sub>4</sub>. Then, the solvent was removed. The crude product was purified with flash column chromatography with eluent of petroleum ether and CH<sub>2</sub>Cl<sub>2</sub> (8:1) to give a white solid (yield 87%). <sup>1</sup>H NMR (400 MHz, CDCl<sub>3</sub>, δ): 7.95 (dt, *J* = 7.9,

1.1 Hz, 1H), 7.83 (dt,  $J = 7.5, 0.9$  Hz, 2H), 7.77 (d,  $J = 2.0$  Hz, 1H), 7.74 - 7.39 (m, 10H), 7.36 (dd,  $J = 3.5, 1.0$  Hz, 2H), 7.35 - 7.27 (m, 4H), 7.26 - 7.14 (m, 2H).  $^{13}\text{C}$  NMR (101 MHz,  $\text{CDCl}_3$ ,  $\delta$ ): 147.49, 147.25, 146.97, 139.84, 135.77, 129.27, 128.63, 128.19, 126.07, 125.60, 125.58, 125.55, 124.53, 123.37, 123.04, 120.52, 60.85. HRMS (ESI)  $m/z$ :  $[\text{M} + \text{H}^+]$  calcd for  $\text{C}_{36}\text{H}_{22}\text{F}_4\text{N}_2$ , 558.1719; found, 559.1792.

## SI-2. Photophysical properties of TPA-3

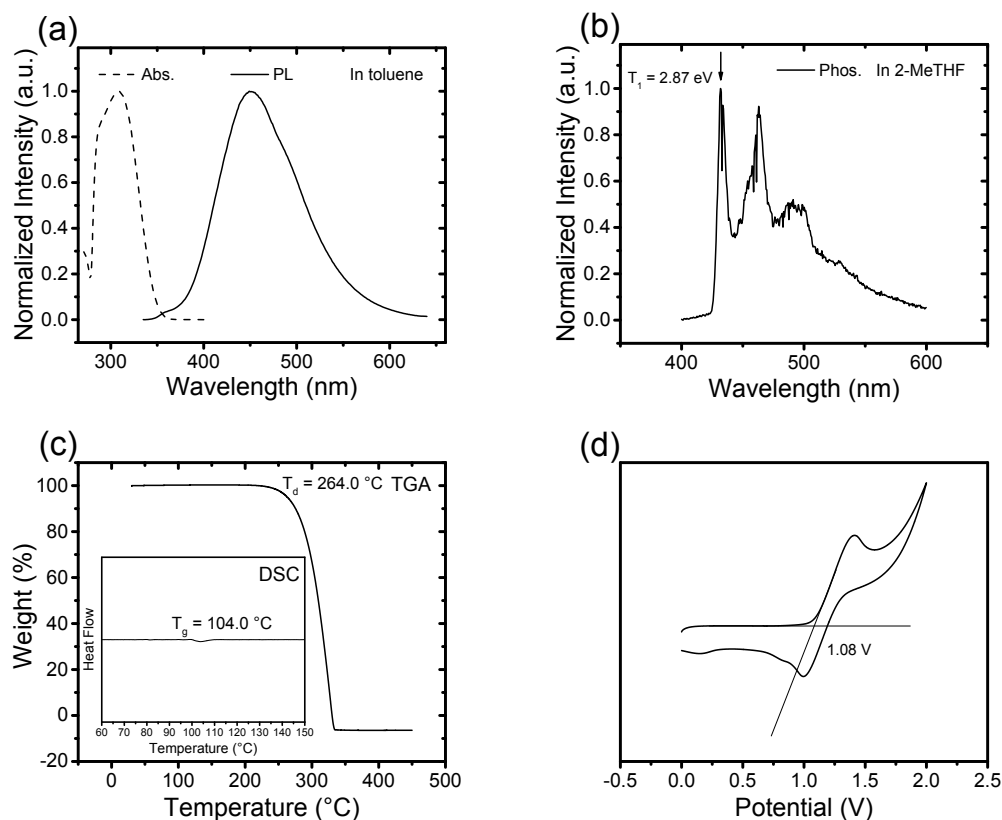


**Figure S1.** (a) UV-vis absorption and PL spectra of TPA-3 in toluene; (b) low temperature (77 K) phosphorescence spectrum of TPA-3 in 2-Me-THF; (c) TGA and DSC (inset) curves of TPA-3; (d) CV curve TPA-3 in  $\text{CH}_2\text{Cl}_2$ .

The photophysical properties of TPA-3 were characterized by ultraviolet-visible (UV-vis) absorption, solution photoluminescence (PL), and low temperature PL measurements. The absorption and PL spectra of TPA-3 in toluene at room temperature are shown in Figure S1a. In the case of PL spectrum, TPA-3 exhibited wide blue emission with peak at 450 nm. From the first peak of the PL emission of TPA-3 in 2-methyl tetrahydrofuran (2-MeTHF) at 77 K, triplet energy of was calculated to be 2.87 eV. Thermal properties were characterized by thermogravimetric analysis (TGA) and differential scanning calorimetry (DSC) under a nitrogen atmosphere at a heating rate of  $20\text{ }^\circ\text{C min}^{-1}$  (Figure S2c in Supporting Information). The decomposition temperature ( $T_d$ , 5% weight loss), glass-transition temperature ( $T_g$ ) and melting temperature ( $T_m$ ) of TPA-3 were measured to be 264.0, 104.0 and 168.2  $^\circ\text{C}$ ,

respectively. Cyclic voltammetry (CV) was conducted to evaluate the HOMO level of TPA-3 because the exciplex emission is known to be correlated with the HOMO level of electron donor material. From the onset of the oxidation potential curve with respect to ferrocene (HOMO = - (4.8 +  $E_{ox}$ ) eV), the HOMO level was determined to be -5.52 eV. The energy gap ( $E_g$ ) of TPA-3 was estimated to be 3.57 eV from the absorption onset. The LUMO level was further calculated to be -1.95 eV.

### SI-3. Low temperature (77 K) phosphorescence spectrum

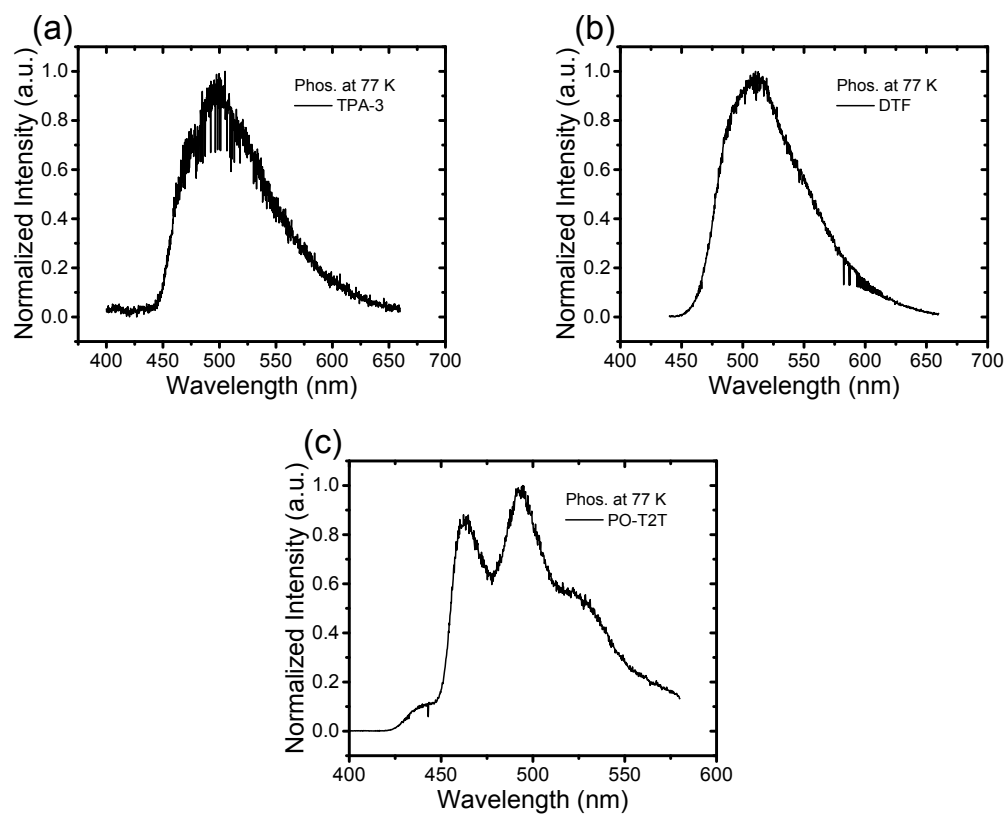


**Figure S2.** Low temperature (77 K) phosphorescence spectrum of (a) TPA-3 film; (b) DTF film; (c) PO-T2T film.

#### SI-4. HOMO, LUMO, and excited state energies

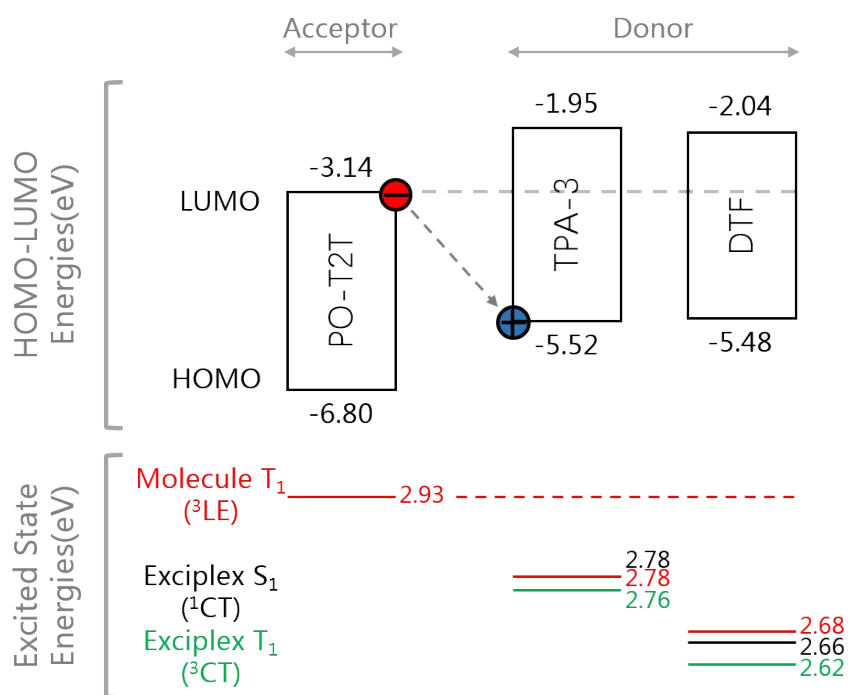


**Figure S3.** HOMO, LUMO, and excited state energies of of TPA-3, DTF, PO-T2T and the exciplex systems.

## SI-5. Vacuum deposited devices

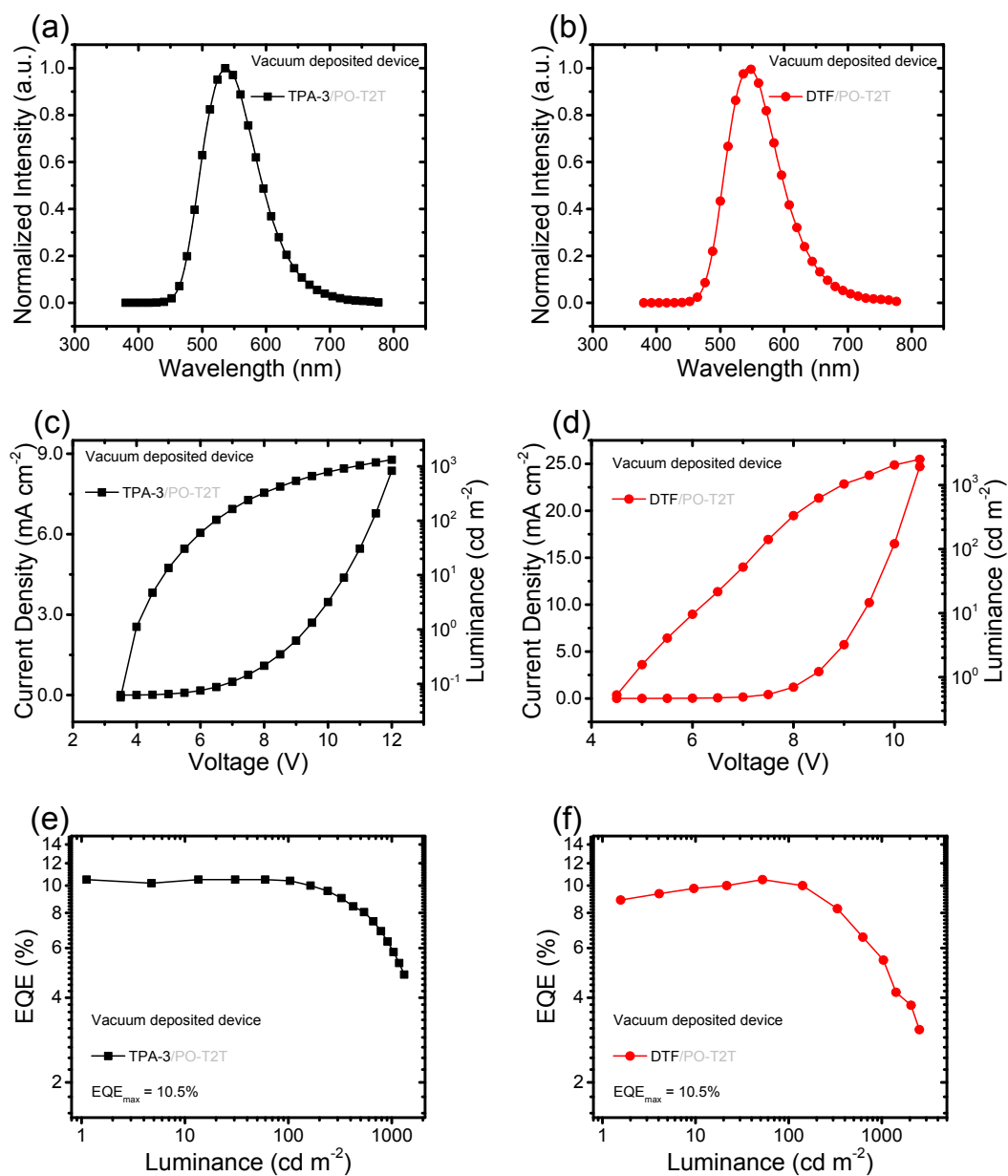


**Figure S4.** J-V-L curves of vacuum deposited devices using (a) TPA-3 and (b) DTF as EMLs; EL spectra of devices using (c) TPA-3 and (d) DTF as EMLs; EQE curves of devices using (e) TPA-3 and (f) DTF as EMLs; configuration of vacuum deposited device: ITO/TAPC (40 nm)/EML (40 nm)/PO-T2T (60 nm)/LiF (0.8 nm)/Al (80 nm).



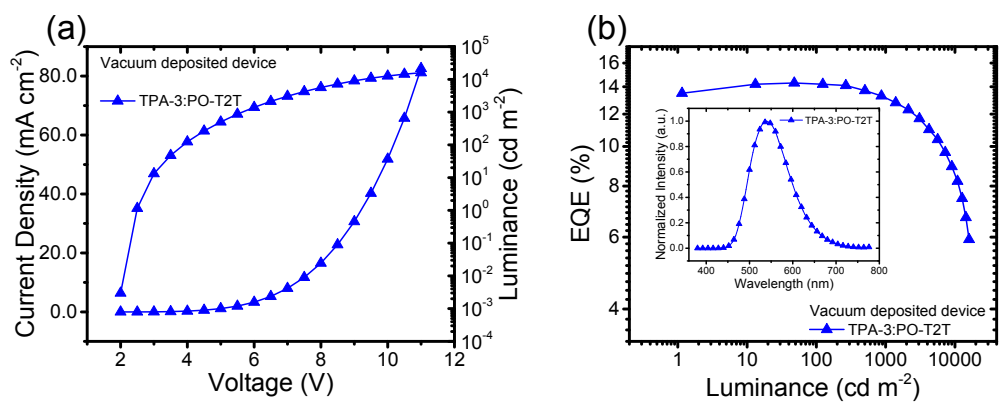


**Figure S5.** (a) J-V-L curves; (b) EQE curves and EL spectra (inset) of vacuum deposited bulk OLEDs using TPA-3:PO-T2T as EML; configuration of vacuum deposited device: ITO/TAPC (40 nm)/TPA-3 (10 nm)/TPA-3:PO-T2T (30 nm)/PO-T2T (60 nm)/LiF (0.8 nm)/Al (80 nm).

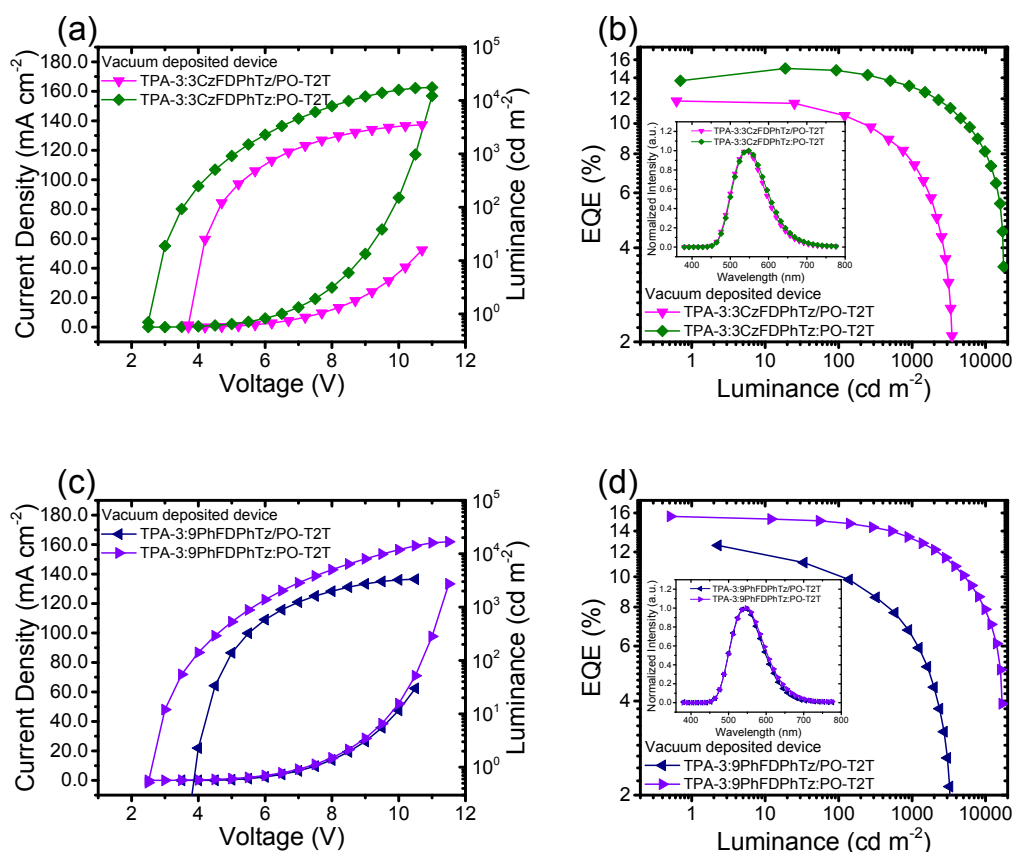


**Figure S6.** (a) J-V-L curves; (b) EQE curves and EL spectra (inset) of vacuum deposited OLEDs using TPA-3:3CzFDPhTz (interfacial exciplex) and TPA-3:3CzFDPhTz:PO-T2T (bulk exciplex) as EMLs; (c) J-V-L curves; (d) EQE curves and EL spectra (inset) of vacuum deposited OLEDs using TPA-3:9PhFDPhTz (interfacial exciplex) and TPA-3:9PhFDPhTz:PO-T2T (bulk exciplex) as EMLs; configuration of vacuum deposited device: ITO/TAPC (40 nm)/TPA-3 (10 nm)/EML (30 nm)/PO-T2T (60 nm)/LiF (0.8 nm)/Al (80 nm).

**Table S1.** Summary of device performances.

EML	Method	$V_{on}$ [V] <sup>a)</sup>	CE/PE/EQE [ $\text{cd A}^{-1}/\text{lm W}^{-1}/\%$ ]		
			Maximum	500 [ $\text{cd m}^{-2}$ ]	1000 [ $\text{cd m}^{-2}$ ]
TPA-3/PO-T2T <sup>b)</sup>	Solution	2.4	44.8/41.5/13.5	35.9/24.4/10.7	17.9/10.8/5.5
	Vacuum	4.0	34.9/25.8/10.5	27.0/9.3/8.2	19.6/5.4/6.0
DTF/PO-T2T <sup>b)</sup>	Solution	2.3	19.7/24.7/6.0	14.3/9.9/4.2	5.3/3.3/1.6
	Vacuum	4.8	35.0/17.7/10.5	24.2/8.9/7.3	18.4/6.3/5.5
TPA-3:PO-T2T <sup>c)</sup>	Solution	3.9	49.1/33.4/14.4	44.3/24.5/13.0	37.3/20.0/11.0
	Vacuum	2.5	47.1/53.6/14.3	45.2/28.4/13.7	43.4/23.8/13.2
TPA-3:3CzFDPhTz/PO-T2T <sup>b)</sup>	Solution	3.1	63.0/43.0/18.8	43.7/26.8/13.1	29.6/16.3/8.9
	Vacuum	3.8	38.1/31.2/11.8	29.0/15.9/8.8	24.8/11.3/7.6
TPA-3:3CzFDPhTz:PO-T2T <sup>c)</sup>	Solution	4.5	59.3/33.2/17.7	51.6/28.4/15.4	40.8/20.7/12.2
	Vacuum	2.5	49.1/54.4/15.0	45.1/31.6/13.7	43.0/26.1/13.1
TPA-3:9PhFDPhTz/PO-T2T <sup>b)</sup>	Solution	3.1	78.2/61.4/24.0	51.8/38.4/15.5	32.7/24.7/10.1
	Vacuum	3.9	40.7/32.0/12.6	26.1/14.1/8.0	21.2/9.6/6.5
TPA-3:9PhFDPhTz:PO-T2T <sup>c)</sup>	Solution	3.8	70.8/44.4/21.4	66.3/41.0/19.8	47.5/30.2/14.5
	Vacuum	2.6	50.0/53.5/15.6	45.9/29.2/14.0	43.5/23.9/13.3

<sup>a)</sup> Estimated at the brightness of  $1 \text{ cd m}^{-2}$ ; <sup>b)</sup> devices utilizing interfacial exciplexes; <sup>c)</sup> devices utilizing bulk exciplexes.

## SI-6. Investigation on turn voltage

For interfacial exciplex OLEDs (TPA-3/PO-T2T), holes and electrons transport to the TPA-3/PO-T2T interface (recombination zone) and recombine to generate excitons for emission. While in the case of bulk exciplex, the recombination of holes and electrons would mainly happen in TPA-3:PO-T2T blend film. Thus, more energy will be needed to overcome the injection barrier from electron-transporting layer to the TPA-3:PO-T2T blend film. To further confirm this explanation, bulk exciplex OLED with the configuration of ITO/PEDOT:PSS/TPA-3:PO-T2T/TmPyPb/LiF/Al was further fabricated. In this device, the recombination zone is completely in the TPA-3:PO-T2T blend film. As shown in Figure S7, TmPyPb-based OLED exhibits the same maximum EQE of 14.4% and turn on voltage of 3.9 V with PO-T2T-based bulk exciplex OLED. Therefore, the increasing of turn on voltage may come from electron injection process from ETL to EML.

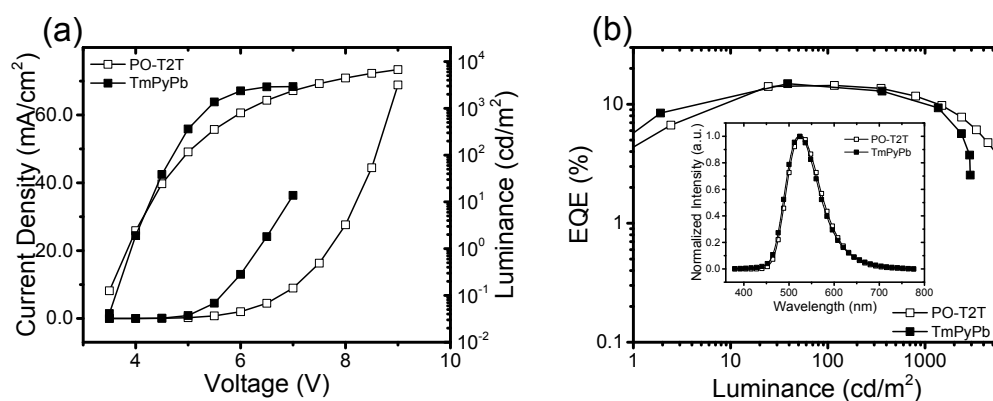


**Figure S7.** (a) J-V-L curves; (b) EQE curves and EL spectra (inset) of bulk OLEDs using PO-T2T and TmPyPb as ETL.

## SI-7. Photophysical properties of 3CzFDPhTz:PO-T2T and 9PhFDPhTz:PO-T2T

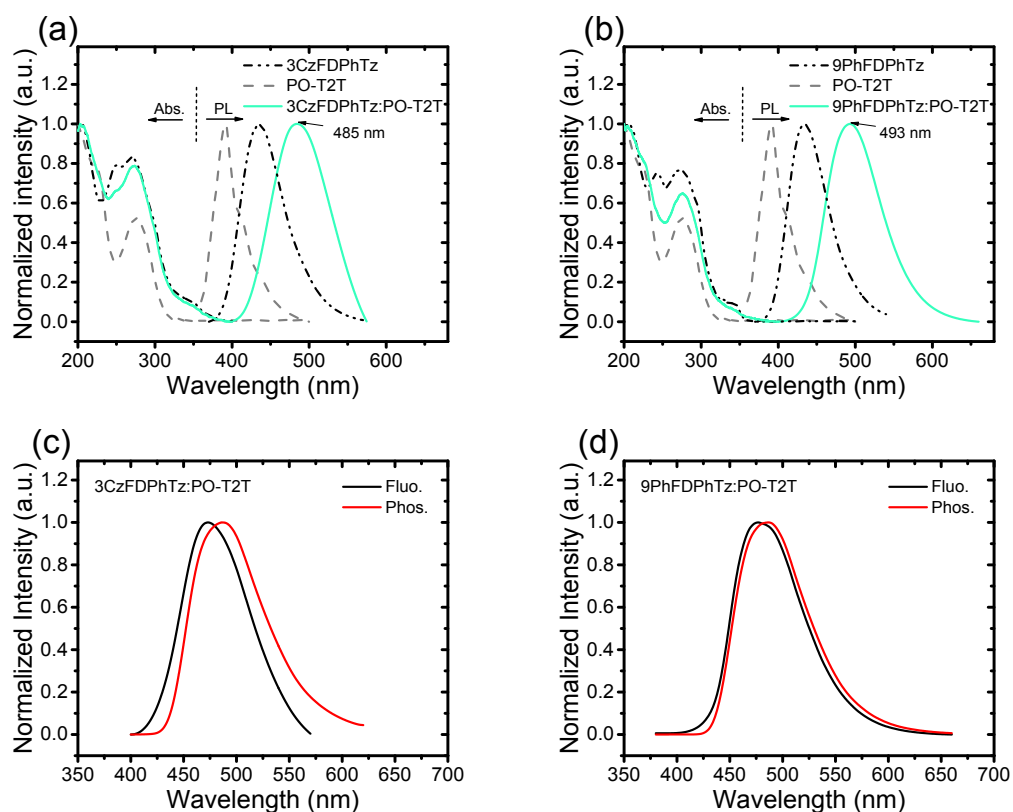


**Figure S8.** (a) UV-vis absorption and PL spectra of 3CzFDPhTz, PO-T2T and 3CzFDPhTz:PO-T2T in solid films; (b) UV-vis absorption and PL spectra of 9PhFDPhTz, PO-T2T and 9PhFDPhTz:PO-T2T in solid films; (c) fluorescence and phosphorescence spectra of 3CzFDPhTz:PO-T2T in solid films at 77 K; (d) fluorescence and phosphorescence spectra of 9PhFDPhTz:PO-T2T in solid films at 77 K.

## SI-8. Calculation of rate constants of different kinetic processes

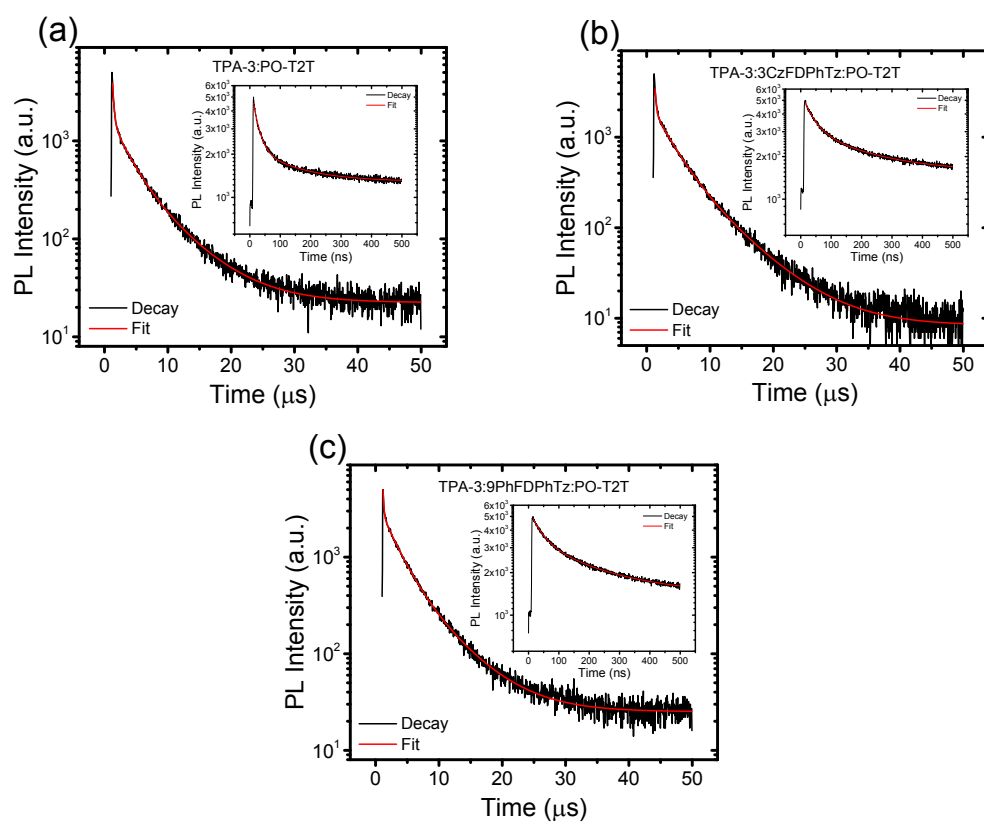


**Figure S9.** Transient PL decay curves of (a) TPA-3:PO-T2T; (b) TPA-3:3CzFDPhTz:PO-T2T; and (c) TPA-3:9PhFDPhTz:PO-T2T films at 300 K.

**Table S2.** Photophysical Data for TPA-3:PO-T2T and TPA-3:9PhFDPPhTz:PO-T2T films.

Exciplex	$\Phi$	$\Phi_p$	$\Phi_d$	$k_p (\times 10^7 \text{ s}^{-1})$	$k_d (\times 10^5 \text{ s}^{-1})$	$K_{\text{risc}} (\times 10^5 \text{ s}^{-1})$	$\Phi_{\text{isc}}$	$\Phi_{\text{risc}}$
TPA-3:PO-T2T	0.57	0.16	0.41	5.05	2.48	7.52	0.84	0.49
TPA-3:3CzFDPPhTz:PO-T2T	0.84	0.13	0.71	2.78	2.20	13.47	0.87	0.82
TPA-3:9PhFDPPhTz:PO-T2T	0.85	0.10	0.75	2.59	2.34	19.45	0.90	0.84

$$k_p = \frac{1}{\tau_p} \quad (\text{S1})$$

$$k_d = \frac{1}{\tau_d} \quad (\text{S2})$$

$$\Phi = \Phi_p + \Phi_d \quad (\text{S3})$$

$$\Phi_p = \frac{A_1 \tau_p}{A_1 \tau_p + A_2 \tau_d} \Phi \quad (\text{S4})$$

$$\Phi_d = \frac{A_2 \tau_d}{A_1 \tau_p + A_2 \tau_d} \Phi \quad (\text{S5})$$

$$k_{\text{isc}} = k_p (1 - \Phi_p) \quad (\text{S6})$$

$$k_{\text{risc}} = \frac{k_p k_d \Phi_d}{k_{\text{isc}} \Phi_p} \quad (\text{S7})$$

$$\Phi_{\text{isc}} = \frac{k_{\text{isc}}}{k_p} \quad (\text{S8})$$

$$\Phi_{\text{risc}} = \frac{\Phi_d}{\Phi_{\text{isc}} (\Phi_p + \Phi_d)} \quad (\text{S9})$$

in which the  $k_p$ ,  $k_d$ ,  $k_{\text{isc}}$ ,  $k_{\text{risc}}$ ,  $\Phi_{\text{isc}}$ ,  $\Phi_{\text{risc}}$  are the prompt fluorescent rate, delayed fluorescent rate, intersystem crossing rate, reverse intersystem crossing rate, intersystem crossing efficiency, reverse intersystem crossing efficiency.

